Available online at www.sciencedirect.com
ScienceDirect
Journal of Magnetic Resonance 189 (2007) 20–31
JMR Journal of Magnetic Resonance
www.elsevier.com/locate/jmr

Pursuing structure in microcrystalline solids with independent molecules in the unit cell using ^{1}H–^{13}C correlation data

James K. Harper, Mark Strohmeier, David M. Grant *

Department of Chemistry, University of Utah, 315 South 1400 East, Salt Lake City, UT 84112, USA

Received 4 May 2007
Available online 14 August 2007

Abstract

The ^{1}H–^{13}C solid-state NMR heteronuclear correlation (HETCOR) experiment is demonstrated to provide shift assignments in certain powders that have two or more structurally independent molecules in the unit cell (i.e. multiple molecules per asymmetric unit). Although this class of solids is often difficult to characterize using other methods, HETCOR provides both the conventional assignment of shifts to molecular positions and associates many resonances with specific molecules in the asymmetric unit. Such assignments facilitate conformational characterization of the individual molecules of the asymmetric unit and the first such characterization solely from solid-state NMR data is described. HETCOR offers advantages in sensitivity over prior methods that assign resonances in the asymmetric unit by ^{13}C–^{13}C correlations and therefore allows shorter average analysis times in natural abundance materials. The ^{1}H–^{13}C analysis is demonstrated first on materials with known shift assignments from INADEQUATE data (santonin and $Ca(OAc)_2$ phase I) to verify the technique and subsequently is extended to a pair of unknown solids: (+)-catechin and $Ca(OAc)_2$ phase II. Sufficient sensitivity and resolution is achieved in the spectra to provide assignments to one of the specific molecules of the asymmetric unit at over 54% of the sites.
© 2007 Elsevier Inc. All rights reserved.

Keywords: Heteronuclear correlation; Powders; Asymmetric unit

1. Introduction

Structural characterization of microcrystalline powders can be a formidable challenge. Numerous analysis techniques are applicable to powders but most explore only particular structural features or properties [1–4]. In contrast, modern X-ray powder diffraction and solid-state NMR (SSNMR) techniques are capable of providing full structures with atom level resolution. Despite the ever-increasing abilities of these techniques, however, many materials remain difficult to characterize. Among these materials are solids that contain more than one molecule per crystallographic asymmetric unit. The asymmetric unit is the smallest unique building block needed to generate the unit cell and is denoted by the symbol Z'. When Z' is >1, the multiple molecules differ structurally with minor variations usually observed in bond lengths and angles. Hence, the individual molecules of the asymmetric unit are frequently described as inequivalent or independent molecules in the SSNMR literature. Quantifying the occurrence of $Z' > 1$ in powders is difficult because no structural databases comparable to the Cambridge Structural Database exist for SSNMR data and the number of powder diffraction structures that have been solved is somewhat limited [5]. However, in our laboratory nearly 30% of the powders analyzed in the past decade have displayed lattices with $Z' > 1$ [6–13]. While this is significantly higher than the 8.3% estimated in general single crystal organic solids [14], it appears to be more typical of solids that involve hydrogen bonds [15]. Indeed, a survey of monoalcohol structures in the Cambridge Structural Database has demonstrated that nearly 40% of the structures examined have $Z' > 1$ [16]. It is therefore important to develop techniques

* Corresponding author. Fax: +1 801 581 8433.
E-mail address: grant@chem.utah.edu (D.M. Grant).

1090-7807/$ - see front matter © 2007 Elsevier Inc. All rights reserved.
doi:10.1016/j.jmr.2007.06.017

capable of reliably providing structure in these materials. Herein, we describe a SSNMR method to aid characterization of solids that contain more than one molecule per asymmetric unit. This work addresses a key step in analyzing spectra of such solids; the ability to assign SSNMR chemical shifts to a distinct molecule of the asymmetric unit when Z' is >1. Such assignments permit subsequent conformational analysis of the individual members of the asymmetric unit and a characterization of this type is described.

2. Results and discussion

2.1. Solid-state NMR methodology

In SSNMR spectra of microcrystalline solids with $Z' > 1$ a single molecular position may give different isotropic signals for each molecule in the asymmetric unit. This creates spectra that are difficult to interpret as illustrated by the ^{13}C spectrum of calcium acetate (Fig. 1). Here, the asymmetric unit contains 4 independent acetates and therefore, rather than the 2 lines observed in solution, 8 are observed in the spectrum (i.e. 4 each for the respective carboxylate and methyl carbons). Complete structural characterization of the 4 acetates of the asymmetric unit requires that each pair of lines from a single molecule of the asymmetric unit be unraveled from the other three. In other words, shifts must be assigned to a specific molecule of the asymmetric unit. Spectroscopically, this task is particularly difficult because the distinct molecules of the asymmetric unit have only minor structural differences and therefore only small shift differences at a given site. Since the set of resonances from a single position are all correlated to identical neighboring atoms, typical multidimensional correlation NMR experiments will inevitably contain sets of closely spaced peaks. Hence, even in spectra with very few signals, the requirements for spectral resolution are high. Despite these difficulties, shifts have previously been assigned to the asymmetric unit with SSNMR using through-bond methods that rely on J-coupling between correlated atom pairs, such as INADEQUATE [17,18] or UC2QF-COSY [19], or spin diffusion methods that transfer magnetization through space via dipolar coupling [20]. To date it appears that five organic products with $Z' > 1$ have been successfully assigned by these methods [21–26]. These techniques usually require either isotopically enriched materials or relatively small natural abundance molecules to ensure success. A third approach provides the most probable assignments by comparing SSNMR shift data with computed shifts for model compounds [8]. Naturally, this latter method is based on statistical probabilities rather than direct experimental evidence. An alternative method is the ^{1}H–^{13}C heteronuclear correlation experiment (HETCOR).

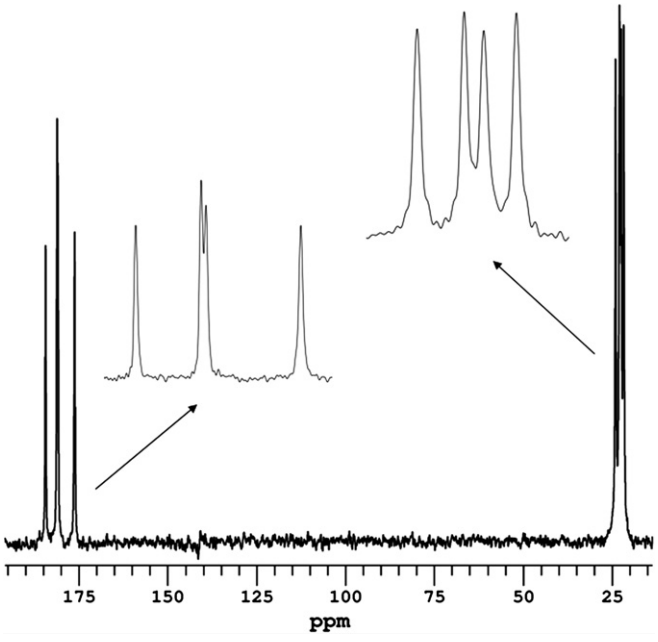

Fig. 1. A ^{13}C spectrum of calcium acetate illustrating the multiple resonances present for each position when the number of molecules in the asymmetric unit (Z') is >1. The phase shown has $Z' = 2$ with 4 independent acetates, thus 8 lines are observed rather than the two found in solution. The spectrum displayed corresponds to phase I ($Ca(OAc)_2{\cdot}0.5H_2O$) described herein.

The ^{1}H–^{13}C HETCOR experiment takes advantage of the 99.99% natural abundance and high gamma of ^{1}H to improve sensitivity over ^{13}C–^{13}C correlation experiments in natural abundance materials. Thus, this technique provides shorter experimental times and access to higher molecular weight molecules. Several variants of the heteronuclear correlation experiment presently exist [27–33] and all function by transferring magnetization from the ^{1}H to the ^{13}C either through bonds or through space. In an early application of this technique van Rossum et al. observed that a 3D version of the HETCOR could differentiate two structurally distinct forms of bacteriochlorophyll c that were simultaneously present [34]. Since the individual molecules of the asymmetric unit have structural differences similar to those seen in the two forms of bacteriochlorophyll c, it is likely that the heteronuclear correlation experiment will provide sufficient ^{1}H resolution to provide assignments to the asymmetric unit.

2.2. Assigning shifts to the asymmetric unit with ^{1}H–^{13}C correlations

Before the HETCOR experiment can be adopted as a method capable of assigning shifts to the asymmetric unit, HETCOR assignments must be verified using compounds with known shifts. Natural abundance calcium acetate ($Z' = 2$ with 4 independent acetates) and santonin (Fig. 2, $Z' = 2$) were therefore evaluated using the solid-state INADEQUATE technique to obtain assignments to the asymmetric unit. INADEQUATE is a relatively insensitive experiment because it monitors adjacent ^{13}C–^{13}C pairs which reduces the sensitivity by a factor of approximately

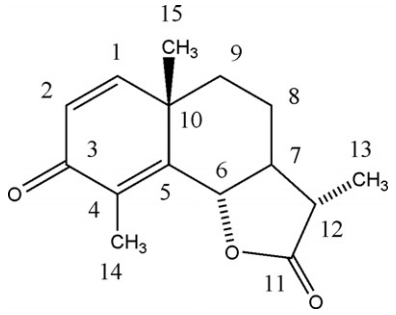

Fig. 2. Structure of santonin showing the numbering used.

100 over 1D spectra in natural abundance samples. The signal intensity is further reduced by long preparation times and the detection or refocusing of antiphase magnetization. For compounds with short homogeneous and heterogeneous T_2, the signal is prohibitively low. This insensitivity is also problematic when analyzing molecules with $Z' > 1$ because only in relatively small molecules can the number of moles analyzed be made high enough to ensure success. Indeed, in prior work with $Z' > 1$, the INADEQUATE approach has only been successfully used when the molecular weight was <400 g/mol. Fortunately, calcium acetate and santonin are particularly well suited for INADEQUATE because both have relatively low molecular weights, and both have long T_2 and short T_1 relaxation times. In both molecules all ^{13}C–^{13}C connections were unambiguously established by the INADEQUATE and assignments are included in Tables 1 and 2.

Comparison to the INADEQUATE data was carried out using a HETCOR experiment that involves magnetization transfer through space via dipolar couplings. This method has the advantage of providing ^{1}H–^{13}C correlations in regions of the molecule that are several bonds removed from a proton. However, the pulse sequence employs a conventional (Hartman-Hahn) cross-polarization step that, potentially, allows ^{1}H homonuclear couplings to become encoded in the data. Prior studies have demonstrated that contact times <250 μs minimize these ^{1}H–^{1}H interactions during cross-polarization[28,34]. Hence, only data with contact times ⩽250 μs were used to minimize $^{1}H \rightarrow {}^{1}H \rightarrow {}^{13}C$ relayed transfers and $^{1}H \rightarrow {}^{13}C$ transfers between two or more molecules in the lattice. Other heteronuclear correlation experiments [27–33] are available including sequences the suppress ^{1}H–^{1}H spin exchange during cross-polarization. Use of these techniques may provide enhanced resolution and sensitivity.

Analysis of calcium acetate is especially straight forward as the only source of protons for magnetization transfer is the methyl group. Additionally, the methyl and carboxylate resonances are assigned easily by their isotropic shifts. The solid analyzed first is denoted as phase I to distinguish it from a second form that is described below. An initial ^{1}H–^{13}C correlation was performed with a 70 μs contact time to allow only magnetization transfer between protons covalently attached to carbons. Prior work has demonstrated that contact times <100 μs provide such transfers as the primary correlations observed [35]. This experiment identifies protonated carbons and provides an assessment of the ^{1}H resolution. In the cases of phase I, the methyl protons are highly degenerate, and only the methyl at 24.95 ppm has sufficient proton resolution to provide assignments in the asymmetric unit. A second dataset with a 200 μs cross-polarization time allowed magnetization transfer to the carboxylate moieties and identified the ^{13}C signals at 24.95 and 186.26 ppm as spatially close and most likely indicate bonded atoms in the asymmetric unit (Fig. 3). Admittedly, this choice of contact time leaves unresolved questions regarding intermolecular transfers and relayed transfers. Discussion of such effects is deferred to the next section where an evaluation of the correlations in santonin is given. Santonin contains many more correlations than calcium acetate and therefore, more general conclusions can be reached from analysis of the santonin HETCOR data. The HETCOR assignment obtained was verified by a comparison to INADEQUATE data shown in Table 1. The individual acetates of the asymmetric unit are denoted by the letters A, B, C and D. Low ^{1}H resolution prevents assignment of the three remaining acetates from the HETCOR data.

A better measure of the ability of the HETCOR analysis to differentiate the separate molecules of the asymmetric unit is provided by santonin ($Z' = 2$). The greater structural diversity of santonin is, however, offset by the fact that the two molecules of the asymmetric unit have nearly identical conformations (Fig. 4). This similarity implies the potential for ^{1}H degeneracy as seen with calcium acetate. Inspection of the ^{1}H–^{13}C correlation data for santonin (Fig. 5) shows that, indeed, only 4 molecular positions

Table 1
A comparison of INADEQUATE and HETCOR ^{1}H and ^{13}C shift assignments in calcium acetate phase I

Position	Molecule A		Molecule B		Molecule C		Molecule D	
	$\delta^{13}C$	$\delta^{1}H$	$\delta^{13}C$	$\delta^{1}H$	$\delta^{13}C$	$\delta^{1}H$	$\delta^{13}C$	$\delta^{1}H$
	^{13}C INADEQUATE							
CH_3	24.52	—	26.00	—	23.75	—	24.95	—
COO^-	178.08	—	182.82	—	183.02	—	186.26	—
	^{1}H–^{13}C HETCOR							
CH_3	—	2.29	—	2.29	—	2.25	24.95	2.41
COO^-	—	—	—	—	—	—	186.26	—

Table 2
A comparison of chemical shift assignments in santonin obtained from solid-state INADEQUATE and HETCOR analyses

Position	INADEQUATE		HETCOR				Correlations ($^1H \rightarrow {}^{13}C$) and ^1H–^{13}C distances (Å)[a]
	Molecule A	Molecule B	Molecule A		Molecule B		
	$\delta^{13}C$	$\delta^{13}C$	δ ^{13}C	δ^1H	$\delta^{13}C$	δ^1H	
1	159.2	158.1	159.2	4.0	158.1	3.9	C1–**H** to 42.3[b] (2.20 Å), 42.5[b] (2.19 Å), 125.2[c] (2.10 Å), 126.1[c] (2.09 Å)
2	125.2	126.1	125.2	2.8	126.1	3.2	C2–**H** 159.2[b] (2.12 Å), 158.1[b] (2.11 Å), 185.9[c] (2.16 Å), 186.9[c] (2.18 Å)
3	185.9	186.9	185.9	—	186.9	—	—
4	127.1	128.3	—	—	—	—	—
5	153.8	153.8	—	—	—	—	—
6	80.8	81.4	80.8	2.5	81.4	2.6	C6–**H** to 42.3[b] (2.72 Å), 42.5[b] (2.72 Å), 54.2[b] (2.15 Å), 54.0[b] (2.15 Å), 40.4[b] (2.71 Å), 39.5[b] (2.72 Å), 26.3[c] (2.67 Å), 25.9[c] (2.70 Å), 23.1[d] (2.68 Å), 21.9[d] (2.66 Å), 177.0[d] (2.76 Å), 178.4[d] (2.77 Å)
7	54.2	54.0	54.2	1.1	54.0	1.1	—
8	23.1	21.9	23.1	1.0	21.9	1.2	—
9	36.6	42.6	—	0.9, 1.4[e]	—	1.0[e]	—
10	42.3	42.5	42.3	—	42.5	—	—
11	177.0	178.4	177.0	—	178.4	—	—
12	40.4	39.5	40.4	1.0	39.5	1.6	C12–**H** to 177.0[b] (2.11 Å), 178.4[b] (2.11 Å)
13	13.7	13.7	—	0.9[e]	—	0.9[e]	—
14[f]	14.2	11.9	—	1.2[e]	—	1.2[e]	—
15	26.3	25.9	26.3	1.0	25.9	0.9	—

The symbols *b*, *c* and *d* denote correlations that were, respectively, best observed at 80, 110 and 150 μs cross-polarization contact times.

[a] The reported ^1H–^{13}C distances were obtained from the X-ray structure. No hydrogen positions were reported for this structure, therefore hydrogens were added and their atomic positions refined at the B3LYP/D95* level of theory.

[e] These ^1H assignment to the A or B molecules of the asymmetric unit were made using ^{13}C assignments from INADEQUATE.

[f] The ^1H at C14 displayed strong correlations to C3, C4 and C5 at a 110 μs contact time, but degeneracy of the C14 protons prevented shift assignments to the asymmetric unit.

(i.e. C1, C2, C6 and C12) have ^1H resonances resolved from other protons. At all remaining positions ^1H degeneracy prevents assignment. Despite this limitation, the 4 resolved ^1H's display correlations that provide assignments for 10 carbons (Fig. 6). Equally satisfying, all HETCOR assignments match those obtained from INADEQUATE data (Table 2).

An X-ray structure is known for santonin, providing the ^1H–^{13}C distances corresponding to each correlation. Evaluating these distances is necessary to determine if the observed correlations are intermolecular or intramolecular in origin. These distances also help assess the contribution from $^1H \rightarrow {}^1H \rightarrow {}^{13}C$ relayed transfers at the contact times employed. In santonin, all observed correlations can be associated with intramolecular ^1H–^{13}C distances $\leqslant$2.77 Å as summarized in Table 2. Because these correlation can consist of a major component of heteronuclear (^1H–^{13}C) dipolar coupling and a minor homonuclear (^1H–^1H) contribution, this technique does not provide ^1H–^{13}C distances of the accuracy reported by van Rossum et al. [28] of ±0.07 Å or less. Even so, the HETCOR results obtained are semi-quantitative. For example, most correlations observed at contact times $\leqslant$110 μs correspond to ^1H–^{13}C distances <2.5 Å, while the 4 additional peaks that appear at a contact time of 150 μs all have ^1H–^{13}C distances >2.6 Å. Thus, these data remain useful for certain conformational analyses.

While short contact times reduce relayed transfers in santonin, evidently a limited amount still takes place even at 80 μs. This appears in the $^1H6 \rightarrow {}^{13}C10$ correlation. In this case, the intramolecular ^1H–^{13}C distance is 2.72 Å in both molecules of the asymmetric unit indicating little potential for magnetization transfer at 80 μs. In fact, nearly identical ^1H–^{13}C intramolecular separations are found at $^1H6$–$^{13}C8$ and $^1H6$ to $^{13}C11$ and these sites undergo transfers that are only observed at 150 μs. However, the ^1H at C6 is only 2.11 Å from a ^1H at C15 that allows a relayed $^1H6 \rightarrow {}^1H15 \rightarrow {}^{13}C10$ transfer. Clearly, this path also gives rise to a $^1H6 \rightarrow {}^1H15 \rightarrow {}^{13}C15$ transfer and thus a $^1H6 \rightarrow {}^{13}C15$ correlation is observed at an unexpectedly short contact time. A third long-range correlation is observed at 80 μs between $^1H6$ and $^{13}C12$ despite ^1H–^{13}C intramolecular separations of 2.71 and 2.72 Å in the A and B molecules, respectively. In this case, the origin of the transfer is less apparent. Possible contributors include an intramolecular path involving $^1H6 \rightarrow {}^1H12 \rightarrow {}^{13}C12$. The small $^1H6/{}^1H12$ separation of 2.62 Å indicates that some transfer should occur. A second intermolecular $^1H6/{}^1H12$ contact of 3.9 Å is also present in the lattice. The observed correlation therefore appears to be a combination of intramolecular relayed and intermolecular transfers.

Inspection of two additional HETCOR datasets acquired for santonin using contact times of 200 and 250 μs did not reveal any new correlations over those found at shorter times. Thus, the majority of the observed correlations (8 out of 11) exhibit no intermolecular or intramolecular relayed correlations. Santonin is somewhat unusual in terms of ^1H–^1H separation because the presence of

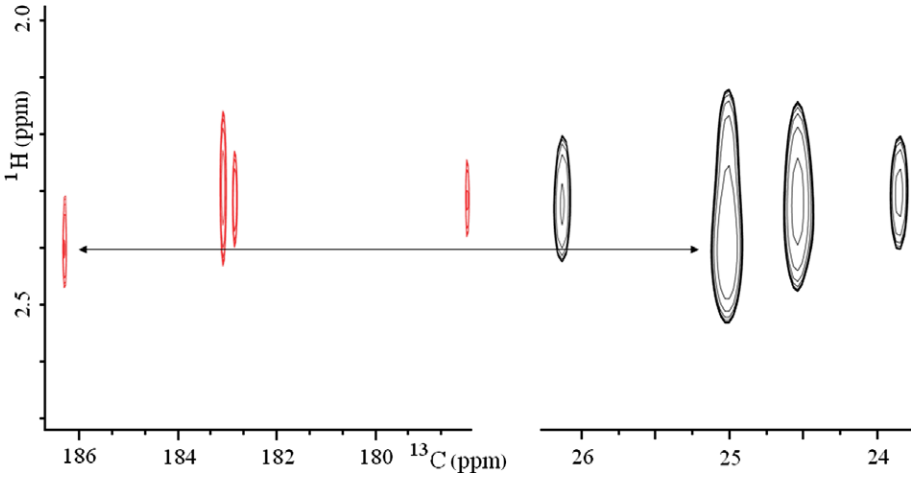

Fig. 3. The ^{1}H–^{13}C HETCOR spectrum (200 μs contact time) of calcium acetate ($Z' = 2$ with 4 independent acetates) showing through-space ^{1}H–^{13}C magnetization transfer between the methyl (the four contours at the right) and the carboxylate atoms (the left four peaks shown as red contours on the web). The short contact time allows only transfers over a few Å and indicates that signals aligned with a given proton shift represent bonded carbons. Resolution is only sufficient to identify peak pairings between the methyl at 24.9 ppm (δ^{13}C) and the carboxylate at 186.3 ppm. This pairing is independently verified by INADEQUATE data. HETCOR assignments for the remaining 3 molecules of the asymmetric unit were not obtained due to a ^{1}H degeneracy of the methyl protons shown above. The two ^{13}C regions of the spectrum displayed are plotted with different vertical scales to allow for clear visual comparison of the data. These contour slices were taken near the tops of the signals to allow identification of peak positions, thus the ^{1}H linewidths shown are not representative of the full width at half of the maxima.

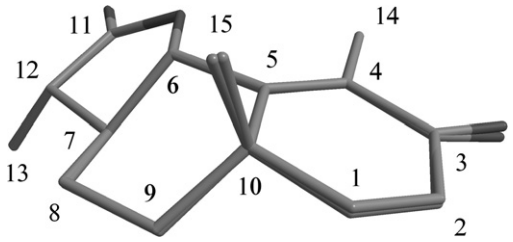

Fig. 4. The two molecules constituting the asymmetric unit of santonin superimposed to illustrate their close structural similarities. Despite the nearly identical conformations, the ^{1}H–^{13}C HETCOR data provide assignments to the asymmetric unit for 10 of the 15 positions.

multiple rings creates steric crowding between protonated regions. Hence, it appears that in less sterically congested compounds HETCOR data collected with contact times of 250 μs or less will show even fewer relayed and intermolecular transfers and may be used with a minimal risk of error.

2.3. Extending ^{1}H–^{13}C heteronuclear correlation methods to unknowns with $Z' > 1$

Analysis of santonin and calcium acetate verifies the ability of HETCOR to provide accurate assignments even in solids where the molecules of the asymmetric unit are nearly identical. However, both these molecules are rigid and give nearly optimal spectra with narrow lines and short T_1 relaxation times. It is crucial that more general solids be evaluated to determine if the HETCOR technique can be successfully applied. In particular, it is important to investigate if the correlations observed can also provide conformational information for the individual members of the asymmetric unit.

A fortuitous decomposition of the calcium acetate sample provided a first test for HETCOR in an unknown lattice. During data collection, sample drying created approximately 20% of a second phase with $Z' = 2$ and four independent acetates as indicated by a ratio of roughly 1:1:1:1 for the 4 new carboxylate peaks formed. This phase, denoted as phase II, had narrow lines suggesting crystallinity, but the amount of material present was insufficient for INADEQUATE analysis. Fortunately, high signal-to-noise correlations were observed in the HETCOR data. In contrast to phase I, this form had sufficient ^{1}H resolution to provide complete assignments for all 4 acetates in the asymmetric unit (Table 3).

The sample of calcium acetate was prepared from water therefore the observation of water HO–^{1}H → ^{13}C peaks should also be evident in the spectrum. Such correlations may allow ordering of the water present and permit prediction of certain lattice features. In the present case, however, no correlations from water protons were observed. The absence of such peaks may result from the short contact times used that permit only short-range transfers or from motion in the water molecules.

Presently, two polymorphs of calcium acetate are known and each has the composition $Ca(OAc)_2{\cdot}H_2O$ [36,37]. A comparison of the NMR samples examined here to these forms was made by growing crystals by slow evaporation from water. Small needle-shaped crystals were obtained and removed from the solution while water was still present to ensure a match to conditions reported in the X-ray diffraction analysis [36]. This form is expected to correspond

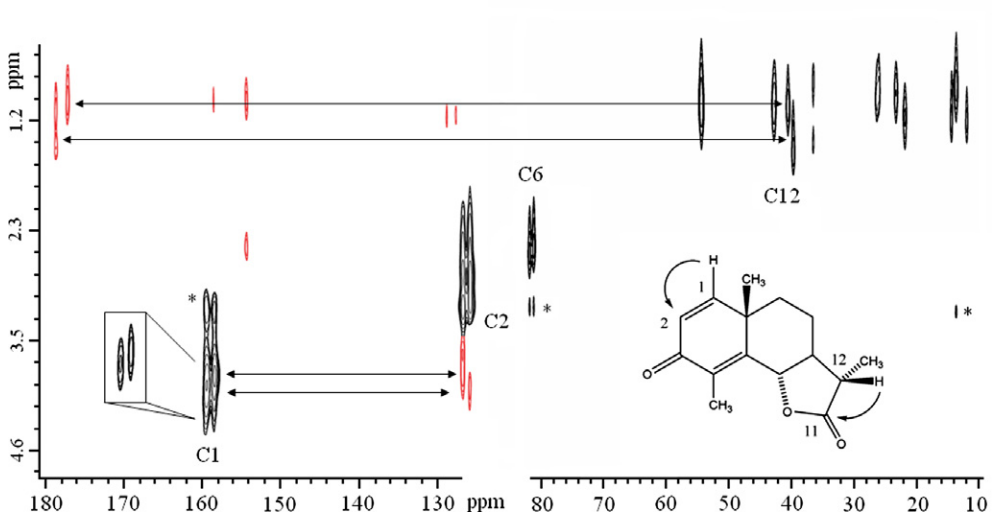

Fig. 5. A ^{1}H–^{13}C correlation spectrum of santonin (200 μs) showing protons directly attached to carbons (black) and signals receiving magnetization from nearby protons (red). Only the protons on carbons 1, 2, 6 and 12 are separated sufficiently to provide reliable assignments to the asymmetric unit. The horizontal arrows indicate two such assignments that correspond to the interactions shown on the included structure. Eight additional assignments (not shown) are also obtained from C1, C2 and C6 as summarized in Fig. 6 and Table 2. The C1 expanded region shows a contour cut near the peak maximum to illustrate the ^{1}H shift differences present. Unsuppressed ^{1}H carrier signal is indicated with an asterisk.

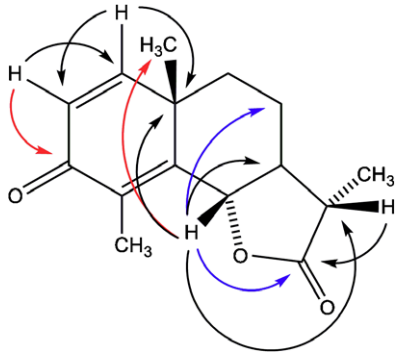

Fig. 6. The ^{1}H–^{13}C correlations, observed in santonin, that provide assignments to the asymmetric unit. The black, red and blue arrows indicate, respectively, correlations best observed at 80, 110 and 150 μs. All shift assignments are given in Table 2.

to $Ca(OAc)_2{\cdot}H_2O$, but analysis by 1D ^{13}C NMR revealed two forms present, each with $Z' = 2$ (Fig. 7). The $Ca(OAc)_2{\cdot}H_2O$ form is identified in this spectrum by the observation that certain peaks decreased upon sample drying over 2 days. A second phase increased as the sample dried and is therefore less hydrated. Complete drying of the sample over several days at room temperature resulted in a spectrum containing only the second form. Elemental analysis demonstrated that this second phase is $Ca(OAc)_2{\cdot}0.5H_2O$ (see Section 4). The NMR sample designated herein as phase I corresponds to $Ca(OAc)_2{\cdot}0.5H_2O$ while phase II appears to be a less hydrated polymorph. Neither phase I nor II correspond to any known crystal structure.

A HETCOR analysis was also performed on a sample of the flavonoid catechin (Fig. 8, $Z' = 2$). The wide-spread natural occurrence of this product and its superb antioxidant properties [38–40] and other bioactivities [41] has made it the subject of extensive study. Catechin's simple structure and general rigidity might appear to make it a favorable target for crystallographic studies, however, no crystal structure is presently available. Accordingly, solid-state characterization is of interest. All ^{1}H and ^{13}C shifts for catechin were first assigned to specific molecular positions by ^{1}H–^{13}C correlations observed at 70, 120, 200 and 250 μs cross-polarization times (Table 4). A doubling of isotropic (1D) ^{13}C lines was observed at several positions suggesting the potential to subsequently assign to the asymmetric unit. At positions 2, 3, 4, 2′ and 6′, correlations were observed that provided such assignments in the asymmetric unit as summarized in Table 5. It is notable that both C2 and C6′ produce broad ^{13}C lines with no discernable doubling in either peak, inferring an inability to assign to the asymmetric unit. However, the C2 protons from the two different molecules of the asymmetric unit are nearly baseline resolved, thus correlations of these protons to C6′ provided assignments to the asymmetric unit for C2 and C6′. The listing of two different ^{13}C shifts for these sites in Table 4 is thus derived from the HETCOR data and not observed in the isotropic data. Isotropic degeneracy in the two $^{1}H8$ signals prevented assignment of the C8 carbon to the asymmetric unit. Likewise position 4a could not be assigned because the only observable correlations are with the ^{1}H signals at C4 which are nearly degenerate.

Conformational information may also be extracted from the HETCOR data. In catechin the correlations of

Table 3
The ^{1}H and ^{13}C shift assignments in phase II of calcium acetate from HETCOR data

Position	Molecule A		Molecule B		Molecule C		Molecule D	
	$\delta^{13}C$	$\delta^{1}H$	$\delta^{13}C$	$\delta^{1}H$	$\delta^{13}C$	$\delta^{1}H$	$\delta^{13}C$	$\delta^{1}H$
CH_3	24.28	2.41	24.76	2.33	25.26	2.44	26.68	2.30
COO^-	183.54	—	184.20	—	187.60	—	176.24	—

$^{1}H2$–$^{13}C6'$ (120 μs contact time) indicates an orientation of the aromatic ring having the C6′ near the C2 proton. Correlations of $^{1}H2$–$^{13}C2'$ are also observed in both molecules of the asymmetric unit, but these are much weaker than the $^{1}H2$–$^{13}C6'$ signals and are only observed at a longer contact time of 250 μs. Thus, the C2′ appears to be oriented away from the C2 proton. The conformation consistent with this result is shown in Fig. 9. This structure assumes an H–C2–C1′–C6′ dihedral angle of 0° because eclipsed conformations are usually energetically preferred about C–C bonds involving sp^3 and sp^2 carbons [42]. Both molecules of the asymmetric unit exhibit these correlations with nearly equal intensity, suggesting that both structures have approximately the same conformation at this position.

Catechin displayed certain correlations in regions of the ^{1}H spectrum that did not correspond to any protons attached to carbon. These correlations are consistent with magnetization transfer arising from OH protons to ^{13}C's and correlations from such protons to C2, C3, C6 (or C8), C2′, C4′ and C5′ were observed (Table 4). These correlations facilitate investigation of hydrogen bonding and in characterizing OH hydrogen conformations. In catechin, the strong correlation from the 4′-$O^{1}H$ to $^{13}C5'$ at 70 μs in only one of the molecules of the asymmetric unit ($\delta^{13}C = 121.68$ ppm) suggests a structure with the OH hydrogen directed toward the C5′. Prior work has demonstrated that phenolic OH protons almost invariably lie in the plane of the aromatic ring [43]. Thus, a structure having the 4′-$O^{1}H$ proton coplanar with the aromatic ring and directed toward C5′ is consistent with these observations (Fig. 10I). In the second molecule of the asymmetric unit ($\delta^{13}C5' = 128.40$ ppm), the absence of this 4′-$O^{1}H$–$^{13}C5'$ correlation indicates a 4′-$O^{1}H$ directed toward the C3′ position and coplanar with the ring as illustrated in structure II of Fig. 10. This proposed difference in the 4′-$O^{1}H$ orientations for the two molecules of the asymmetric unit is likely the origin of the large isotropic difference between the two C5′ resonances in the asymmetric unit ($\Delta = 6.72$ ppm). The C2′ position also exhibits large isotropic differences for the two molecules of the asymmetric unit ($\Delta = 6.59$ ppm) nearly identical to that observed at C5′. As with C5′, this difference is consistent with 3′-$O^{1}H$ orientations that differ by 180° as shown in Fig. 10 I and II. However, only weak correlations are observed between the 3′-$O^{1}H$ and $^{13}C2'$ at a 70 μs contact time making direct conformational verification difficult.

Fortunately, independent support for the C3′ and C4′ OH conformations, proposed in Fig. 10, is available from steric considerations. Prior work on both solid anisole [44] and 1,4-dihydroxybenzene (quinol) [45] has established that steric interactions between the OR moiety (R = H or CH_3) and the neighboring hydrogens, shown in Fig. 11, create large shift differences between the C2 and C6 positions. The C3 and C5 sites of quinol are equivalent to C6 and C2, respectively, and thus equally influenced. In anisole, this steric interaction moves the C2 shift upfield by 7.0 ppm relative to C6. This pattern is also observed in quinol, but the shift difference is smaller ($\Delta = 1.8$ ppm). Hence, in catechin the aromatic C–H that interacts sterically with the OH proton should display the lower frequency shift. Indeed, in the HETCOR data the 4′-$O^{1}H$ to $^{13}C5'$ correlation involves the smaller C5′ shift

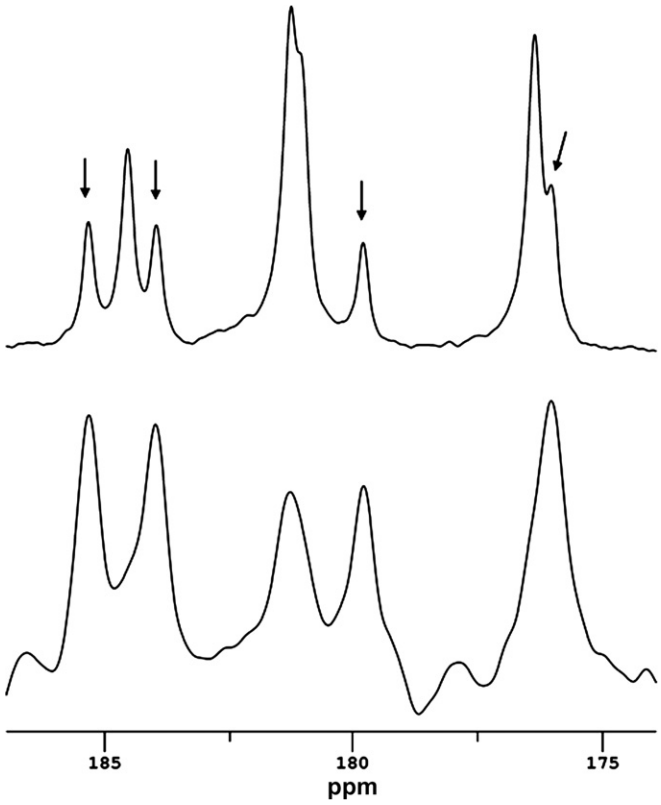

Fig. 7. An expansion of the ^{13}C carboxylate region of calcium acetate after crystallization from water. The lower spectrum was taken while the sample was still moist and contains two phases with $Z' = 2$ and 4 independent acetates, as more clearly distinguished in the upper plot. The top spectrum is the same sample after drying for 2 days in a rotor at room temperature with occasional sample spinning (4 kHz). The peaks marked by arrows are seen to decrease upon drying and thus correspond to $Ca(OAc)_2{\cdot}1H_2O$. The peaks observed to increase in the upper plot (no arrows) represent a less hydrated form and correspond to phase I described herein ($Ca(OAc)_2{\cdot}0.5H_2O$ by elemental analysis).

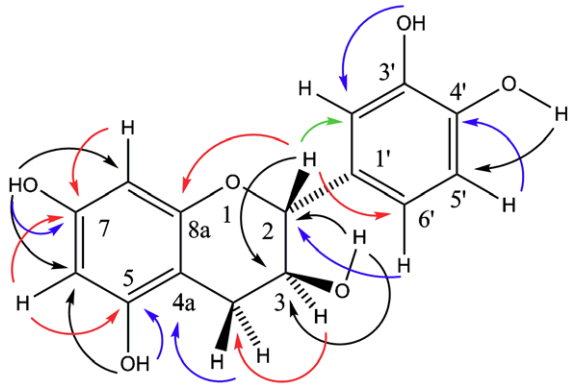

Fig. 8. The ^{1}H–^{13}C correlations observed in catechin using 70 μs (black arrows), 120 μs (red), 200 μs (blue) and 250 μs (green) cross-polarization times. Correlation of protons to covalently attached carbons are also observed in all cases, but are omitted here for clarity. The ^{1}H resolution at C2 and C3 are sufficient to provide assignments to the asymmetric unit at carbons 2, 3, 4, 2′ and 6′. Carbon 5′ was also assigned to the asymmetric unit from steric considerations described in the text. At all other positions, assignments to molecular positions are provided, but no assignments to the asymmetric unit were made. All shift assignments are given in Table 4.

($\delta^{13}C = 121.68$ ppm), as predicted. These steric considerations also support the 3′-OH conformations shown in Fig. 10 and predict that structure II should be associated with the smaller C2′ shift of 111.82 ppm. In catechin, this steric effect creates shift differences that are surprisingly large and comparable in magnitude to those observed in anisole.

These steric considerations also allow the C5′ shifts of catechin to be assigned to the asymmetric unit (Table 5). This is possible because C2′ is assigned from HETCOR data and the C5′ shifts can be paired with the C2′ shifts through the steric effects.

The correlation from the OH proton at C3 also provides conformational information. Specifically, in both molecules of the asymmetric unit, 3′-O^{1}H to ^{13}C2 correlations of nearly equal intensity are observed at 70 μs. This indicates an orientation of this proton towards C2 in both members of the asymmetric unit. An H–O–C3–C2 dihedral angle of +60° or −60° is proposed (Fig. 12) because such staggered conformations are usually energetically preferred about C–O bonds involving an sp^3 carbon [46]. An unambiguous prediction of the H–O–C3–C2 dihedral angle is not possible from the experimental data, however, because any dihedral angle of $+\theta$ will have an identical 3-O^{1}H–^{13}C2 distance at $-\theta$. No conformational predictions can be made for the OH's at C5 and C7 due to both ^{1}H and ^{13}C near degeneracy at C6 and C8.

3. Conclusions

The spectral complexity created by multiple molecules per asymmetric unit presently hampers structural analysis of certain powders by solid-state NMR. The ^{1}H–^{13}C HETCOR analyses, described herein, remedy some of the difficulties by providing shift assignments to specific molecules of the asymmetric unit in natural abundance samples. This technique has a sensitivity advantage over alternative methods that correlate low abundance nuclei. However, sufficient resolution in the ^{1}H and ^{13}C resonances corresponding to the independent molecules of the asymmetric unit is required for unambiguous assignment. High ^{1}H resolution is often difficult to achieve, especially for the multiple members of the asymmetric unit. Yet, in the 4 samples evaluated here, assignments to the asymmetric unit were obtained at over 54% of the carbon positions. Recently reported improvements in ^{1}H line widths [47,48] portend an even greater ability to assign future samples.

Table 4
Carbon and ^{1}H shift assignments in (+)-catechin

Position	$\delta^{13}C$ (ppm)	$\delta^{1}H$ (ppm)	Correlations $^{1}H \rightarrow {}^{13}C$
2	82.97, 83.36	1.8, 2.9	C2–**H** to C3, C8a, C2′ and C6′
3	67.86, 69.53	2.0, 2.8	C3–**H** to C4
		1.3 (C3O–H)	C3O–**H** to C2 and C3
4	31.46, 30.41	1.6, 1.7	C4–**H** to C4a
4a	100.40, 102.13	—	—
5[a]	154.01	1.1 (C5O–H)	C5O–**H** or C7O–**H** to C6 or C8
6[b]	96.82	2.8[c]	C6–**H** to C5 and C7
7[a]	154.01	1.1 (C7O–H)	C5O–**H** or C7O–**H** to C6 or C8
8[b]	97.55, 97.93	2.9, 2.9	C8–**H** to C7
8a	154.97	—	—
1′	129.95	—	—
2′	111.82, 118.41	3.5, 3.5	—
3′	144.08	2.2 (C3′O–H)	C3′O–**H** to C2′
4′	145.68	2.3 (C4′O–H)	C4′O–**H** to C5′
5′	121.63, 128.40	4.2	C5′–**H** to C4′
6′	121.68, 121.29	4.3	C6′O–**H** to C2

[a] These assignments cannot be unambiguously determined due to ^{1}H and ^{13}C degeneracy. The assignments shown are therefore interchangable.
[b] Unequivocal assignments cannot be made due to near ^{1}H degeneracy and the assignments shown are interchangable.
[c] This ^{1}H signal has a line width greater than other protons in the spectrum and appears to contain contributions from the adjacent OH. The center position of the signal is reported here.

Table 5
Assignment of ^{13}C shifts to the asymmetric unit in solid (+)-catechin from HETCOR data

Position	Molecule A		Molecule B		Correlations ($^1H \rightarrow {}^{13}C$)[a]
	$\delta^{13}C$ (ppm)	δ^1H (ppm)	δ ^{13}C (ppm)	δ^1H (ppm)	
2	82.97	1.8	83.36	2.9	C2–**H** to 67.86, 69.53, 111.82, 118.41, 121.29 and 121.68
3	69.53	2.8	67.86	2.0	C3–**H** to 30.41 and 31.46
4	30.41	1.6	31.46	1.7	—
2′	118.41	3.5	111.82	3.5	—
5′[b]	121.63	4.2	128.40	4.2	—
6′	121.29	4.3	121.68	4.3	—

[a] Correlations included are only those providing assignment to the asymmetric unit.
[b] This assignment was made by analogy to the steric effects observed in anisole and 1.4-dihydroxybenzene.

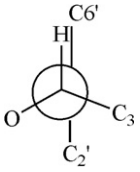

Fig. 9. The HETCOR predicted conformation about the C2–C1′ bond in catechin. The two molecules of the asymmetric unit both display C2–H to C6′ correlations of roughly equal intensity, indicating that both have this conformation.

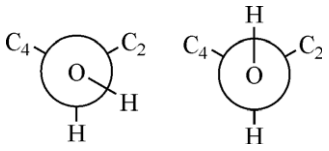

Fig. 12. Predicted conformations for the C2O–H in the two molecules of the asymmetric unit of catechin. Since both structures have nearly identical OH–C2 distances, neither can be eliminated solely from HETCOR data.

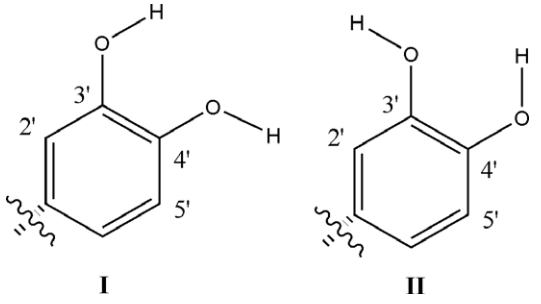

Fig. 10. Proposed conformation of the C3′ and C4′ OH hydrogens in two molecules of the asymmetric unit of catechin.

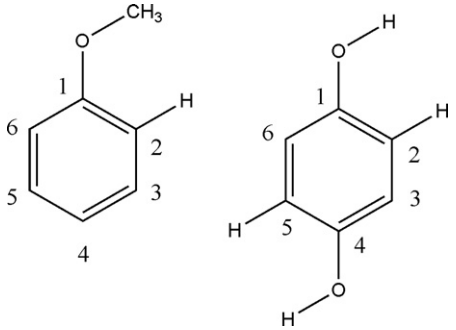

Fig. 11. Structures of anisole of 1,4-dihydroxybenzene (quinol) illustrating the steric influence of OR on aromatic carbons. In both cases, the interaction of the H or CH_3 with the aromatic C–H shown at C2 or C5 (in quinol) result in a upfield shift of roughly 2–7 ppm in the isotropic shift at the C2 (or C5) carbon.

The HETCOR assignments provide information that can be used to assign conformation to the individual molecules of the asymmetric unit. Prior structural analysis of individual members of the asymmetric unit by SSNMR has been accomplished only in conjunction with X-ray diffraction data [21]. In contrast, HETCOR data from catechin provides the first conformational characterization of the individual molecules in the asymmetric unit for a major segment of the structure solely from SSNMR data. These results suggest the potential for complete conformational characterization in larger systems having multiple molecules per asymmetric unit. Extension of this work to such molecules (e.g. taxol with $Z' = 2$) is presently being pursued in our laboratory.

4. Experimental

Samples of (−)-α-santonin and (+)-catechin were purchased from Aldrich and Fluka, respectively, and used as received. Calcium acetate was prepared by adding 0.617 g of calcium hydroxide to 25 mL of water then mixing in 1.0 g of glacial acetic acid dropwise with stirring. Unreacted calcium hydroxide was filtered off after 30 min. Solid calcium acetate was obtained by slow evaporation of the aqueous solution at room temperature to yield a microcrystalline powder corresponding to the NMR sample designated herein as phase I. This solid consisted of a single phase and was stable at room temperature over several weeks with no observable change in the 1D ^{13}C SSNMR spectrum. Elemental analysis of phase I was performed at Atlantic Microlabs (Norcross, GA, USA) and found % C = 28.71 and % H = 4.24. This corresponds to $Ca(OAc)_2{\cdot}0.5H_2O$ which is predicted to have % C = 28.74 and % H = 4.22. Calcium acetate phase II was only formed upon SSNMR analysis for extended periods (i.e. multiple days) and presumably is a result of sample heating during

Table 6
Experimental parameters used in ^{1}H–^{13}C heteronuclear correlation analyses

	Calcium acetate (phase I and II)	Santonin	Catechin
^{13}C spectral width (kHz)	35.997	30.003	25.000
^{1}H spectral width (kHz)	8.698	16.640	26.701
^{13}C frequency (MHz)	150.833903	150.832980	150.831153
^{1}H frequency (MHz)	599.793288	599.796359	599.794560
Spinning speed (kHz)	13.0	11.0	11.0
^{1}H 90° pulse (μs)	2.10	2.13	2.05
Intensity of B_1 (^{1}H) field (kHz)	113.6	108.7	116.3
Number LG cycles per increment	6	4	2
Evolution increments	32	64	64
Scans per increment	128	256	256
Experiment time (h)	28.5	18.3	13.8
Cross-polarization times (μs)	70 and 200	80, 110 and 150	120, 200 and 250
Recycle time (s)	25.0	4.0	3.0

analysis. Efforts to create a sample of only phase II by heating in an oven (70 °C) resulted in a mixture of phase II and several new forms. Thus, all analyses of phase II were performed using a mixture of phase I and II.

All solid-state INADEQUATE experiments were performed on Chemagnetics CMX 200, CMX400 and Varian InfinityPlus 600 spectrometers operating at carbon frequencies of 50.31, 100.62 and 150.83 MHz, respectively. The CMX spectrometers were equipped with dual channel 7.5 mm pencil probes and the Varian spectrometer with a T3 4 mm doubly tuned triple channel probe. The ^{13}C π-pulse widths on the CMX and InfinityPlus spectrometers were 8 and 5.2 μs, respectively. The ^{1}H π-pulse widths were 8 and 5.1 μs, respectively, on the CMX and InfinityPlus systems. In all experiments, transverse ^{13}C magnetization was prepared by CP, and TPPM decoupling was used during preparation, evolution and acquisition time with a phase shift angle of 14°. The INADEQUATE pulse sequence of Lesage et al. [17] was used for all analyses. The preparation time was set to 5 ms in all experiments corresponding to 1/4 J of 50 Hz and a multiple of the rotor period in order to maximize generation of double quantum coherence. Rotary resonance results in an increase in the effective T_2 and hence leads to dramatic reduction in signal intensity. The spinning speed in all experiments was chosen so that rotary resonance conditions between connected peaks were avoided. In order to avoid all possible rotary resonance conditions and to allow for a complete ^{13}C shift assignment of the asymmetric unit in santonin INADEQUATE spectra were recorded at 4.7 T and 14.1 T fields with 6 and 12 kHz spinning speeds, respectively. At 14.1 T the ^{13}C CP rf amplitude was ramped to maximize the magnetization transfer for all carbon positions. The INADEQUATE assignment to the asymmetric unit in $Ca(OAc)_2$ phase I was recorded at 9.4 T field with a spinning speed of 5.0 kHz.

All HETCOR analyses were performed on a wide-bore 600 MHz Varian Infinity spectrometer using a 4.0 mm probe and the pulse sequence of van Rossum et al. [30]. In all spectra, the ^{1}H dimension was referenced to a non-spinning sample of liquid DMSO in a sealed capillary at 2.49 ppm and the ^{13}C dimension was referenced to the high frequency peak of adamantane at 38.56 ppm. All reported proton shifts were scaled by 0.577 as required for Lee-Goldburg homonuclear decoupling [30]. Linear prediction was employed in processing the ^{1}H dimension of all spectra both to replace the first 3 points acquired and also to extend the data points by N/2, where N is the number of directly acquired evolution points. Other acquisition parameters are summarized in Table 6.

All HETCOR spectra were interpreted visually by assigning all carbons correlated with a single proton as ^{13}C sites that are near that proton. Signals from directly bonded protons were identified from a HETCOR analysis performed using very short contact times of <100 μs. The assignments process is simplified by the observation that $^{1}H \rightarrow {}^{13}C$ transfers seldom extend beyond approximately 5 Å, even at contact times as long as 2 ms [35]. Hence, regions of the molecule close to a proton of interest were the primary focus when assigning signals.

Acknowledgments

Funding for this project was provided by the National Institute of Health under Grant 5R01GM08521-44. Dr. Jacalyn S. Clawson in acknowledged for helpful discussions regarding acquisition and analysis of the heteronuclear correlation data.

References

[1] D.R. Vij (Ed.), Handbook of Applied Solid State Spectroscopy, Springer, New York, 2006.
[2] H.G. Brittain (Ed.), Physical Characterization of Pharmaceutical Solids, Marcel Dekker, New York, 1995.
[3] A.R. West, Basic Solid State Chemistry, Wiley, Chichester, 1999.
[4] D. Briggs, Surface Analysis of Polymers by XPS and Static SIMS, Cambridge University Press, Cambridge, 1998.
[5] As of 2006, inclusive, a total of 1328 publications have reported structural determination from powder diffraction as described in the "Structure Determination from Powder Diffraction—Database".
[6] J.K. Harper, D.H. Barich, E.M. Heider, D.M. Grant, R.R. Franke, J.J. Johnson, Y. Zhang, P.L. Lee, R.B. von Dreele, B. Scott, D. Williams, G.B. Ansell, A combined solid-state NMR and X-ray

powder diffraction study of a stable polymorph of paclitaxel, Cryst. Growth Des. 5 (2005) 1737–1742.
[7] J.K. Harper, A.M. Arif, D.M. Grant, cis-Verbenol, Acta Crystallogr. C 56 (2000) 451–452.
[8] J.K. Harper, G. McGeorge, D.M. Grant, Solid-state ^{13}C chemical shift tensors in terpenes. 2. NMR characterization of distinct molecules in the asymmetric unit and steric influences on shift in parthenolide, J. Am. Chem. Soc. 121 (1999) 6488–6496.
[9] J.K. Harper, D.M. Grant, Solid-state ^{13}C chemical shift tensors in terpenes. 3. Structural characterization of polymorphous verbenol, J. Am. Chem. Soc. 122 (2000) 3708–3714.
[10] J.S. Clawson, K.L. Anderson, R.J. Pugmire, D.M. Grant, ^{15}N NMR chemical shift tensors of substituted hexaazaisowurtzitanes: the intermediates in the synthesis of CL-20, J. Phys. Chem. A 108 (2004) 2638–2644.
[11] M. Strohmeier, A.M. Orendt, D.W. Alderman, D.M. Grant, Investigation of the polymorphs of dimethyl-3,6-dichloro-2,5-dihydroxyterephthalate by solid-state NMR spectroscopy, J. Am. Chem. Soc. 123 (2001) 1713–1722.
[12] D.W. Alderman, G. McGeorge, J.Z. Hu, R.J. Pugmire, D.M. Grant, A sensitive, high resolution magic angle turning experiment for measuring chemical shift tensor principal values, Mol. Phys. 95 (1998) 1113–1126.
[13] G. Strobel, E. Ford, J. Worapong, J.K. Harper, A.M. Arif, D.M. Grant, P.C.W. Fung, R.M.W. Chau, Isopestacin, an isobenzofuranone from pestalotiopsis microspora, possessing antifungal and antioxidant activities, Phytochemistry 60 (2002) 179–183.
[14] N. Padmaja, S. Raakmar, A. Viswamitra, Space-group frequency of proteins and of organic compounds with more that one formula unit in the asymmetric unit, Acta Crystallogr. A 46 (1990) 725–730.
[15] A. Gavezzotti, G. Filippini, Geometry of the intermolecular X–H $\cdots$ Y (X,Y = N,O) hydrogen bond and the calibration of the empirical hydrogen-bond potentials, J. Chem. Phys. 98 (1994) 4831–4837.
[16] C.P. Brock, L.L. Duncan, Anomalous space-group frequencies for monoalcohols C_nH_mOH, Chem. Mater. 6 (1994) 1307–1312.
[17] A. Lesage, C. Auger, S. Caldarelli, L. Emsley, Determination of through-bond carbon–carbon connectivities in solid-state NMR using the INADEQUATE experiment, J. Am. Chem. Soc. 119 (1997) 7867–7868.
[18] A. Lesage, M. Bardet, L. Emsley, Through-bond carbon–carbon connectivities in disordered solids by NMR, J. Am. Chem. Soc. 121 (1999) 10987–10993.
[19] L. Mueller, D.W. Elliott, K.C. Kim, C.A. Reed, P.D.W. Boyd, Establishing through-bond connectivity in solids with NMR: structure and dynamics in HC(60)(+), J. Am. Chem. Soc. 124 (2002) 9360–9361.
[20] N.M. Szeverenyi, M.J. Sullivan, G.E. Maciel, Observation of spin exchange by two-dimensional Fourier transform carbon-13 cross polarization-magic angle spinning, J. Magn. Reson. 47 (1982) 462–475.
[21] R.A. Olsen, J. Struppe, D.W. Elliott, R.J. Thomas, L. Mueller, Through-bond ^{13}C–^{13}C correlation at the natural abundance level: refining dynamic regions in the crystal structure of vitamin-D3 with solid-state NMR, J. Am. Chem. Soc. 125 (2003) 11784–11785.
[22] M.T. Zell, B.E. Padden, D.J.W. Grant, S.A. Schroeder, K.L. Wachholder, I. Prakash, E.J. Munson, Investigation of polymorphism in aspartame and neotame using solid-state NMR spectroscopy, Tetrahedron 56 (2000) 6603–6616.
[23] M.T. Zell, B.E. Padden, D.J.W. Grant, M.-C. Chapeau, I. Prakash, E.J. Munson, Two-dimensional high-speed CP/MAS spectroscopy of polymorphs. 1. Uniformly ^{13}C-labeled aspartame, J. Am. Chem. Soc. 121 (1999) 1372–1378.
[24] G. De Paepe, A. Lesage, S. Steuernnagel, L. Emsley, Transverse dephasing optimized NMR spectroscopy in solids: natural abundance ^{13}C correlation spectra, ChemPhysChem 5 (2004) 869–875.
[25] M. Strohmeier, J.K. Harper, D.M. Grant, 45th Experimental NMR Conference 2004, Poster 398.
[26] R.K. Harris, S.A. Joyce, C.J. Pickard, S. Cadars, L. Emsley, Assigning carbon-13 NMR spectra to crystal structures by the INADEQUATE pulse sequence and first principals computation: a case study of two forms of testosterone, Phys. Chem. Chem. Phys. 8 (2006) 137–143.
[27] B. Elena, A. Lesage, S. Steuernagel, A. Böckmann, L. Emsley, Proton to carbon-13 INEPT in solid-state NMR spectroscopy, J. Am. Chem. Soc. 127 (2005) 17296–17302.
[28] B.-J. van Rossum, C.P. de Groot, V. Ladizhansky, S. Vega, H.J.M. de Groot, A method for measuring heteronuclear (^1H–^{13}C) distances in high speed MAS NMR, J. Am. Chem. Soc. 122 (2000) 3465–3472.
[29] E. Vinogradov, P.K. Madhu, S. Vega, Proton spectroscopy in solid state nuclear magnetic resonance with windowed phase modulated Lee-Goldburg decoupling sequences, Chem. Phys. Lett. 354 (2002) 193–202.
[30] B.-J. van Rossum, H. Förster, H.J.M. de Groot, High-field and high-speed CP-MAS ^{13}C NMR heteronuclear dipolar-correlation spectroscopy of solids with frequency-switched Lee-Goldburg homonuclear decoupling, J. Magn. Reson. 124 (1997) 516–519.
[31] S. Hafner, H.W. Spiess, Multiple-pulse line narrowing under fast magic-angle spinning, J. Magn. Reson. A 121 (1996) 160–166.
[32] P.K. Madhu, X. Zhao, M.H. Levitt, High-resolution ^1H NMR in the solid state using symmetry-based pulse sequences, Chem. Phys. Lett. 346 (2001) 142–148.
[33] A. Lesage, D. Sakellariou, S. Steuernagel, L. Emsley, Carbon–proton chemical shift correlation in solid-state NMR by through-bond multiple-quantum spectroscopy, J. Am. Chem. Soc. 120 (1998) 13194–13201.
[34] B.-J. Van Rossum, D.B. Steengaard, F.M. Mulder, G.J. Boender, K. Schaffner, A.R. Holzwarth, H.J.M. de Groot, A refined model of the chlorosomal antennae of the green bacterium Chlorobium tepidum from proton chemical shift constraints obtained with high-field 2-D and 3-D MAS NMR dipolar correlation spectroscopy, Biochemistry 40 (2001) 1587–1595.
[35] J. Brus, A. Jegorov, Through-bond and through-space solid-state NMR correlations at natural isotopic abundance: signal assignment and structural study of simvastatin, Phys. Chem. A 108 (2004) 3955–3964.
[36] E.A. Klop, A. Schouten, P. van der Sluis, A.L. Spek, Structure of calcium acetate monohydrate, $Ca(C_2H_3O_2)_2H_2O$, Acta Crystallogr. C 40 (1984) 51–53.
[37] P. Van der Sluis, A. Schouten, A.L. Spek, Structure of a second polymorph of calcium acetate monohydrate, Acta Crystallogr. C 43 (1987) 1922–1924.
[38] J.S. Wright, E.R. Johnson, G.A. DiLabio, Predicting the activity of phenolic antioxidants: theoretical method, analysis of substituent effects, and application to major families of antioxidants, J. Am. Chem. Soc. 123 (2001) 1173–1183.
[39] Z.Y. Chen, P.T. Chan, K.Y. Ho, K.P. Fung, J. Wang, Antioxidant activity of natural flavonoids is governed by number and location of their aromatic hydroxyl groups, Chem. Phys. Lipids 79 (1996) 157–164.
[40] E.J. Lien, S. Ren, H.-H. Bui, R. Wang, Quantitative structure–activity relationship analysis of phenolic antioxidants, Free Radic. Med. 26 (1999) 285–294.
[41] K. Freudenberg, K. Weinges, in: T.A. Geissman (Ed.), The Chemistry of Flavonoid Compounds, Pergamon Press, 1962, pp. 197–216.
[42] K.B. Wiberg, E. Martin, Barriers to rotation adjacent to double bonds, J. Am. Chem. Soc. 107 (1985) 5035–5041.
[43] J.S. Wright, D.J. Carpenter, D.J. McKay, K.U. Ingold, Theoretical calculation of substituent effects on the O–H bond strength of phenolic antioxidants related to vitamin E, J. Am. Chem. Soc. 119 (1997) 4245–4252.
[44] J.C. Facelli, A.M. Orendt, Y.J. Jiang, R.J. Pugmire, D.M. Grant, Carbon-13 chemical shift tensors and molecular conformation of anisole, J. Phys. Chem. 100 (1996) 8268–8272.

[45] S. Matsui, A. Saika, Study of static and dynamic structure of β-quinol–methanol clathrate by carbon-13 high-resolution solid-state NMR and proton T_1 measurements, J. Chem. Phys. 77 (1982) 1788–1799.

[46] J.P. Lowe, Barriers to internal rotation about single bonds, Prog. Phys. Org. Chem. 6 (1968) 1–80.

[47] B. Elena, G. de Paëpe, L. Emsley, Direct spectral optimization of proton–proton homonuclear dipolar decoupling in solid-state NMR, Chem. Phys. Lett. 398 (2004) 532–538.

[48] E. Vinogradov, P.K. Madhu, S. Vega, Strategies for high resolution proton spectroscopy in solid-state NMR, Top. Curr. Chem. 246 (2005) 33–90.